JOURNAL OF APPLIED PHYSICS **115**, 17C901 (2014)

Novel bias-field-free spin transfer oscillator

Thomas Windbacher,[a)] Alexander Makarov, Hiwa Mahmoudi, Viktor Sverdlov, and Siegfried Selberherr
Institute for Microelectronics, TU Wien, Gußhausstraße 27–29/E360, A-1040 Wien, Austria

(Presented 7 November 2013; received 20 September 2013; accepted 28 October 2013; published online 27 January 2014)

Two versions of magnetic field free spin torque oscillators with in- and out-of-plane spin polarizers are proposed. The field free spin torque oscillators comprise two spin valve stacks with a common free magnetic layer featuring an out-of-plane anisotropy. Their operation frequencies are controlled by the dimensions of the free layer and can also be tuned by the applied currents. Large and stable magnetization precessional motion of the whole shared free layer for both oscillators are obtained. The structure with in-plane polarizers allows more efficient microwave power extraction of the large in-plane magnetization precession of the free layer. *© 2014 AIP Publishing LLC*.
[http://dx.doi.org/10.1063/1.4862936]

I. DEVICE STRUCTURE AND MODEL

Spin torque nanoscale oscillators are very attractive as cost effective on-chip integrated microwave oscillators[1–7] due to their nanoscale size, frequency tunability, broad temperature operation range, and CMOS technology compatibility; however, the need for an external magnetic field limits their practical implementation. Recently, a bias-field-free spin-transfer nano-oscillator was demonstrated.[8] Here, we propose two versions of magnetic field free spin torque oscillators, with in- and out-of-plane spin polarizers, featuring large and stable precessions of the free layer magnetization.

The structure under consideration shown in Fig. 1 consists of two spin valves shearing a common free magnetic layer with a perpendicular magnetization direction described by the out-of-plane uni-axial anisotropy K_1. The magnetization of the free layer can be altered by spin torques generated by the currents flowing through the spin polarizers A and B. First, a perpendicular magnetization of the polarizers' fixed layers is considered. The magnetization of the polarizers is fixed by an anti-ferromagnetic coupling to the pinned layer.[8] A Cartesian coordinate system with a positive z axis along the fixed layers' magnetization is considered. The current applied through valve A generates a torque trying to invert the magnetization of the free layer initially pointing along the positive z direction. The opposite current through valve B generates a torque preserving the initial orientation of the free layer magnetization and thus opposes switching. As a result, a stable precession of the whole free layer is developed. The presence of the second spin valve providing the opposite spin torque distinguishes the oscillator proposed from those studied in Refs. 5–7.

To study the properties of the oscillations, a series of magnetization dynamics simulations has been carried out, for several free layer sizes and different current values. The Landau-Lifshitz-Gilbert equation[9] supplemented with the corresponding torques was employed for analyzing the precessional motions in the shared free layer

$$\frac{d\vec{m}}{dt} = \gamma\left(-\vec{m}\times\vec{H}_{eff} + \alpha\left(\vec{m}\times\frac{d\vec{m}}{dt}\right) + \beta\,\epsilon(\vec{m}\times\vec{p}\times\vec{m} - \epsilon'\,\vec{m}\times\vec{p})\right). \quad (1)$$

Here, $\vec{m}$ denotes the reduced magnetization, $\vec{p}$ is the unit polarization direction of the polarized current, and $\vec{H}_{eff}$ is the effective field which includes the out-of-plane uni-axial magnetic anisotropy, exchange, and demagnetization contributions.[10] The stray fields from the polarizer stacks arranged from anti-ferromagnetically coupled fixed and pinned layers are assumed to be mostly compensated and neglected. The last term in (1) describes the spin transfer torque.[11] The torque term $\beta\epsilon$ is given by

$$\beta\,\epsilon = \frac{\hbar}{\mu_0 e}\,\frac{J}{lM_s}\,\frac{P\Lambda^2}{(\Lambda^2+1)+(\Lambda^2-1)(\vec{m}\cdot\vec{p})}. \quad (2)$$

Here, $\hbar$ is the Planck constant, μ_0 is the vacuum permittivity, e is the electron charge, J is the applied current density, l is the free layer thickness, M_s is the magnetization saturation, P is the polarization, and $\Lambda = 2$. The material and simulation parameters used are summarized in Table I and can be found in Refs. 12 and 13. Simulations were done with help of Ref. 14.

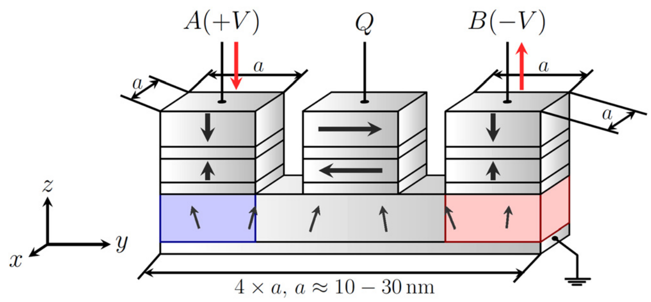

FIG. 1. The current flowing through valve A exerts a spin torque on the shared free layer trying to flip its magnetization direction. At the same time, the second current of opposite polarity flows through valve B and prevents the local magnetization orientation from flipping. The action of both currents results in the magnetization precession of the whole layer.

[a)]Electronic mail: windbacher@iue.tuwien.ac.at. URL: www.iue.tuwien.ac.at.

TABLE I Parameters used for simulations.

Parameter	Value
Free layer thickness l	3 nm
Contact sizes a	$(10\,\mathrm{nm})^2$, $(20\,\mathrm{nm})^2$, $(30\,\mathrm{nm})^2$
Magnetization saturation M_S	4×10^5 A/m
Out-of-plane uni-axial anisotropy K_1	10^5 J/m^3
Uniform exchange constant A_{exch}	2×10^{-11} J/m
Polarization P	0.3
Spin barrier	*Cu*
Gilbert gyromagnetic ratio γ	2.211×10^5 m/A s
Damping constant α	0.01
Non-adiabatic contribution ϵ'	0.1[15]
Λ	2
Discretization length Δx, Δy	2 nm
Discretization length Δz	3 nm
Discretization time Δt	2×10^{-14}s

II. RESULTS

Fig. 2 illustrates the averaged magnetization dynamics of the free layer in the case when the current is flowing only through the valve *A*. Although the torque acts only at a part of the free layer, the magnetization switches its orientation rapidly in the whole layer. Similar behavior was observed in Ref. 12, where it was used to create a majority gate.

If now two currents with identical amplitude but opposing polarity are applied, large and stable magnetization precession appears, as shown in Fig. 3. This is due to the second spin torque exerted in valve B which prevents the layer from switching. The presence of the opposite torque through the valve *B* is crucial for the development of the stable magnetization precession. The oscillations are developed without applying an external magnetic field otherwise needed to achieve precession as in the earlier proposed structures.[5–7] Because of negligible stray fields from the polarizers, the precessions are not localized under the fixed layers, as in Refs. 5–7. The entire layer carries out the precessional movement as illustrated in Fig. 4.

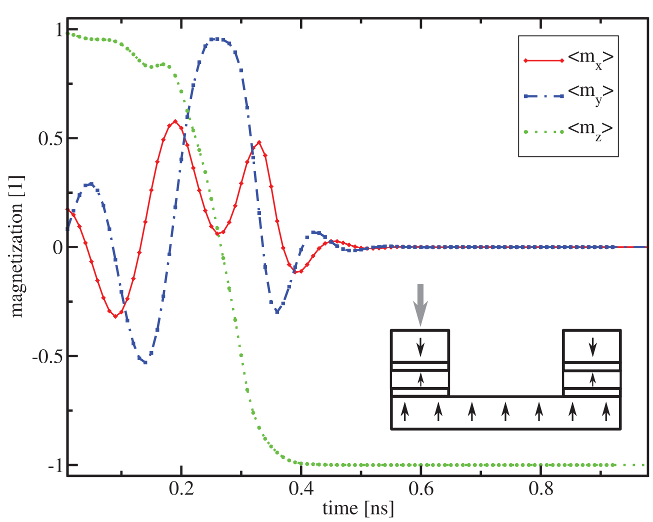

FIG. 2. $\langle m_x(t)\rangle$, $\langle m_y(t)\rangle$, and $\langle m_z(t)\rangle$ for 10 nm × 40 nm and 2×10^{12} A/m^2 current densities in the case of only one input current.

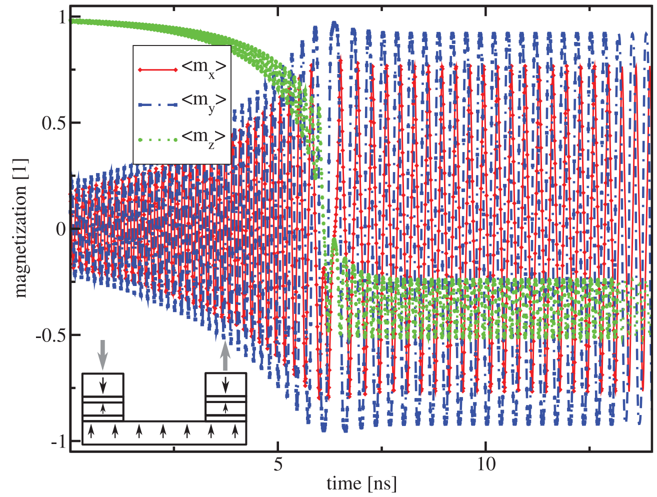

FIG. 3. $\langle m_x(t)\rangle$, $\langle m_y(t)\rangle$, and $\langle m_z(t)\rangle$ for 10 nm × 40 nm and 2×10^{12} A/m^2 current densities in the case of two input currents.

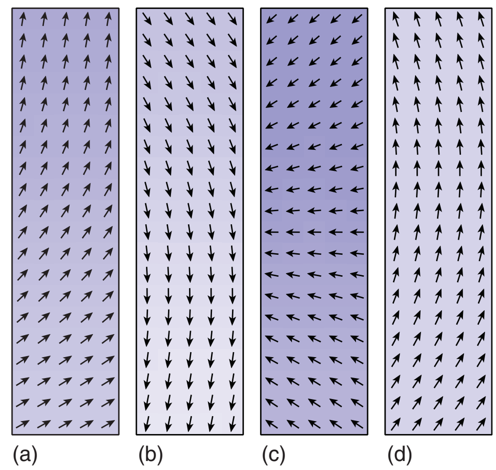

FIG. 4. Temporal xy magnetization dependence for parameters in Fig. 3.

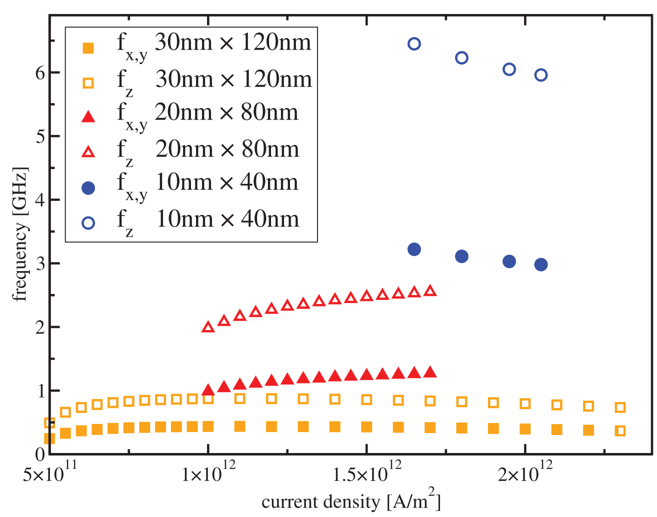

FIG. 5. $f_{x,y}$ describes the in-plane while f_z denotes the out-of-plane component of the oscillations as a function of current density and shared free layer size.

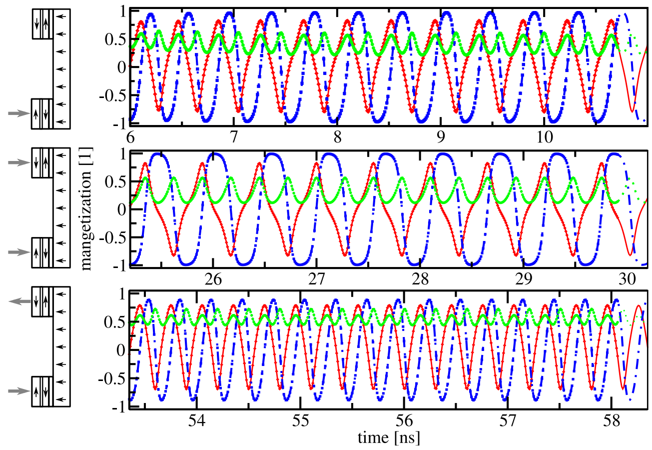

FIG. 6. Applying a current density of $4. \times 10^{11}$ A/m^2 in region A only leads to large and stable precessions (top figure). Adding an identical input current in region B shifts the oscillations to smaller frequencies (middle figure). Inverting the polarity of one input current and cutting the current amplitude in half in region B increases the frequency (bottom figure).

The occurring precessional motion is a superposition of an in-plane precession and an out-of-plane oscillation. For a fixed current density, the frequency f_z for the out-of-plane component oscillations (filled symbols) is two times the corresponding in-plane precession f_{xy} frequency (open symbols). By plotting these two frequencies as functions of current density for different shared free layer sizes, one can see that the precessional frequencies are size dependent (see Fig. 5).

For 30 nm $\times$ 120 nm structure, the stable precessional motion starts at $\approx$250 MHz ($\approx 5 \times 10^{11}$ A/m^2) and goes up to $\approx$450 MHz (1×10^{12} A/m^2), while for 20 nm $\times$ 80 nm the precessions start at $\approx$1 GHz ($1. \times 10^{12}$ A/m^2) and increase to $\approx$1.17 GHz (1.25×10^{12} A/m^2). For 10 nm $\times$ 40 nm, they range from $\approx$3.22 GHz (1.6×10^{12} A/m^2) to $\approx$3. GHz (2.05×10^{12} A/m^2). This appears consistent with geometrically controlled resonance condition, when a shorter free layer length results in a shorter wave length of excitations and higher resonance frequency.

For an electrical microwave power extraction, only the $m_z(t)$ oscillations can be used due to the perpendicular polarizer orientation. Because the oscillations of the free layer are mostly in-plane, the extracted power is small. In order to facilitate a larger power extraction due to bigger $m_{x,y}(t)$ components of the oscillations, one requires a third valve Q with an in-plane polarizer located in between the current injecting spin valves. However, the introduction of an additional stack increases the complexity of the structure. In addition, the maximum power extracted is limited because it is proportional to the power put through valve Q which must be sufficiently small to not disturb the oscillations.

Therefore, we study an alternative setup with in-plane polarizers as recently suggested by Zeng *et al.*[8] Fig. 6 shows that the magnetization in a free layer with perpendicular orientation also exhibits large in-plane precession. In this case, the stable oscillations exist even when the current is driven through a single stack. The current through the second stack allows to modulate the frequency: if the current through the second stack flows in a different direction, the frequency of the oscillations is almost doubled. Because of the in-plane orientations of the polarizers, the microwave power due to the large $m_{x,y}(t)$ component is extracted. In addition, because of the bar shape of the free layer with the excitation sources at its opposite ends the wireless (due to the strong oscillating magnetic field) power sensing, extraction, and further distribution is more convenient in this structure.

III. CONCLUSION

Two versions of magnetic field free spin torque oscillators with in- and out-of-plane spin polarizers featuring large and stable precession are proposed. Its operation frequencies are controlled by the dimensions of a free layer and can also be tuned by the applied currents. The structure with in-plane polarizers allows more efficient microwave power extraction of the large in-plane magnetization precession of the free layer.

ACKNOWLEDGMENTS

This research was supported by the European Research Council through the Grant No. 247056 MOSILSPIN.

[1] L. Berger, Phys. Rev. B **54**, 9353 (1996).
[2] J. Slonczewski, J. Magn. Magn. Mater. **159**, L1 (1996).
[3] M. Tsoi, A. G. M. Jansen, J. Bass, W.-C. Chiang, M. Seck, V. Tsoi, and P. Wyder, Phys. Rev. Lett. **80**, 4281 (1998).
[4] S. I. Kiselev, J. C. Sankey, I. N. Krivorotov, N. C. Emley, R. J. Schoelkopf, R. A. Buhrman, and D. C. Ralph, Nature **425**, 380 (2003).
[5] C. Boone, J. A. Katine, J. R. Childress, J. Zhu, X. Cheng, and I. N. Krivorotov, Phys. Rev. B **79**, 140404 (2009).
[6] G. Finocchio, N. Maugeri, L. Torres, and B. Azzerboni, IEEE Trans. Magn. **46**, 1523 (2010).
[7] D. V. Berkov, C. T. Boone, and I. N. Krivorotov, Phys. Rev. B **83**, 054420 (2011).
[8] Z. Zeng, G. Finocchio, B. Zhang, P. K. Amiri, J. A. Katine, I. N. Krivorotov, Y. Huai, J. Langer, B. Azzerboni, K. L. Wang, and H. Jiang, Sci. Rep. **3**, 1426 (2013).
[9] T. Gilbert, Phys. Rev. **100**, 1243 (1955).
[10] J. E. Miltat and M. J. Donahue, "Numerical micromagnetics: Finite difference methods," in *Handbook of Magnetism and Advanced Magnetic Materials* (John Wiley & Sons, Ltd., 2007).
[11] J. Xiao, A. Zangwill, and M. D. Stiles, Phys. Rev. B **70**, 172405 (2004).
[12] D. Nikonov, G. Bourianoff, and T. Ghani, IEEE Electron Device Lett. **32**, 1128 (2011).
[13] D. Nikonov, G. Bourianoff, and T. Ghani, in *Proceedings of the 11th IEEE Conference on Nanotechnology (IEEE-NANO)* (2011), pp. 1384–1388.
[14] M. Donahue and D. Porter, "OOMMF user's guide, version 1.0," *Interagency Report No. NISTIR 6376, National Institute of Standards and Technology, Gaithersburg, MD*, 1999.
[15] A. V. Khvalkovskiy, K. A. Zvezdin, Y. V. Gorbunov, V. Cros, J. Grollier, A. Fert, and A. K. Zvezdin, Phys. Rev. Lett. **102**, 067206 (2009).